Geosphere

Geologic setting of the Peña de Bernal Natural Monument, Querétaro, México: An endogenous volcanic dome

Gerardo J. Aguirre-Díaz, Alfredo Aguillón-Robles, Margarito Tristán-González, Guillermo Labarthe-Hernández, Margarita López-Martínez, Hervé Bellon and Jorge Nieto-Obregón

Geosphere 2013;9;557-571
doi: 10.1130/GES00843.1

Notes

Geologic setting of the Peña de Bernal Natural Monument, Querétaro, México: An endogenous volcanic dome

Gerardo J. Aguirre-Díaz[1,*], Alfredo Aguillón-Robles[2,*], Margarito Tristán-González[2], Guillermo Labarthe-Hernández[2], Margarita López-Martínez[3,*], Hervé Bellon[4,*], and Jorge Nieto-Obregón[5,*]

[1]*Centro de Geociencias, Universidad Nacional Autónoma de México, campus Juriquilla, Boulevard Juriquilla 3001, Juriquilla, Querétaro, C.P. 76230, México*

[2]*Instituto de Geología, Universidad Autónoma de San Luis Potosí, San Luis Potosí, México*

[3]*División de Ciencias de la Tierra, Centro de Investigación Científica y de Educación Superior de Ensenada, Carretera Ensenada-Tijuana No 3918, Zona Playitas, C.P. 22860, Ensenada, México*

[4]*European University of Brittany, 6538, Domaines Océaniques, Institut Universitaire Européen de la Mer (IUEM), Université de Bretagne Occidentale, 29280 Plouzané, France*

[5]*Facultad de Ingeniería, Universidad Nacional Autónoma de México, Ciudad Universitaria, Delegación Coyoacán, 04510, México, D.F., México*

ABSTRACT

Peña de Bernal is a natural monument located near the town of Bernal, in Querétaro State, central Mexico. It is one of the tallest monoliths of the world, with a maximum height of 433 m. Peña de Bernal was recently declared *Intangible Cultural Heritage of Humanity Patrimony* by United Nations Educational, Scientific, and Cultural Organization (UNESCO). In spite of being both a natural and cultural monument, little is known about its origin, physical characteristics, and chemical composition. It is a leucocratic-igneous rock intruding marine Mesozoic sedimentary rocks and has been misinterpreted as a pluton of Eocene or older age. However, this study shows that Peña de Bernal is a dacitic dome with SiO_2 = 67 wt% and an age of 8.7 ± 0.2 Ma. The complete Peña de Bernal body includes three plugs that crop out in an ~3.5 × 1.5 km area elongated N40°E. Texture of the rock is porphyritic, nearly holocrystalline (80 vol% crystals and 20 vol% glass), with a mineral assemblage of pyroxene, hornblende, biotite, plagioclase, and quartz, plus accessory apatite and zircon. Peña de Bernal dacite is a spine-type endogenous dome that was forcefully intruded through the Mesozoic sequence practically as a solid plug.

*Emails: Aguirre-Díaz: ger@geociencias.unam.mx; Aguillón-Robles: aaguillonr@uaslp.mx; López-Martínez: marlopez@cicese.mx; Bellon: herve.bellon@univ-brest.fr; Nieto-Obregón: nieto@servidor.unam.mx.

INTRODUCTION

Peña de Bernal, at 20°45′N, 99°57′W (Fig. 1), is a prominent peak that was declared a natural reserve area by the State Government of Querétaro in 2007 (Fig. 2). Since 30 September 2009, it has been included in UNESCO's Intangible Cultural Heritage sites (UNESCO, 2009) in order to preserve the traditions of Otomí and Chichimeca indigenous peoples as well as the Peña de Bernal itself. Furthermore, Peña de Bernal is known as the main entrance to the Sierra Gorda mountains area, a range that was declared in 2001 as a Biosphere Reserve by UNESCO (2001). In a few publications and in some web sites, including the official municipal (county) web page of the Bernal area and that of the National Institute of History and Anthropology (INAH) of Mexico, Peña de Bernal is identified as one of the highest monoliths in the world, with monolith defined as a prominent and large monolithologic rock (Fig. 2). The exact height of Peña de Bernal has not been well constrained, with reported heights ranging between 288 and 360 m (e.g., Coenraads and Koivula, 2007; INAH, 2009; Municipio Ezequiel Montes, 2009). From the topographic data of the official Mexican agency for National Geographic Studies and Information (Instituto Nacional de Geografía Estadística e Informática [INEGI], 2002) and from altimeter measurements carried out by us at the base and at the top of Peña de Bernal, we have calculated a height of 433 m on the northern side (Fig. 3). Height is 405 m on the southern side of Peña de Bernal with respect to the plain where Bernal town lies (2049 meters above sea level [masl]). Either elevation chosen from these new values shows that the Peña de Bernal is apparently the highest monolith of the world.

Previous regional geologic mapping has considered Peña de Bernal as a Paleocene monzogranodioritic pluton (Segerstrom, 1961) or a subvolcanic Miocene felsic body (Carrillo-Martínez, 1998). However, the mechanism of emplacement has remained unknown. Before this work, there were no scientific studies specifically on Peña de Bernal's geologic nature and origin. The purpose of this study is therefore to provide detailed information on the geologic setting, including the stratigraphy, structure, geochronology, and geochemistry, to answer fundamental questions of when and how Peña de Bernal was formed and why it is topographically prominent with respect to its surroundings.

GEOLOGY

Peña de Bernal is located at the intersection of three major geologic provinces: the Miocene–Quaternary Mexican Volcanic Belt (Demant, 1978; Aguirre-Díaz et al., 1998; Siebe et al., 2006), the mid-Tertiary Sierra Madre Occidental ignimbrite-dominated sequence (McDowell and Clabaugh, 1979; Aguirre-Díaz et al., 2008), and the Mesozoic Sierra Madre Oriental fold-thrust belt (Suter, 1987; Bartolini et al., 1999), which in this area corresponds to the Sierra Gorda sector (Fig. 1). A simplified geologic map of the Peña de Bernal area is shown in Figure 4. The stratigraphy is briefly described below, from the oldest to the youngest unit (Fig. 5).

Geosphere; June 2013; v. 9; no. 3; p. 557–571; doi:10.1130/GES00843.1; 16 figures; 6 tables.
Received 5 July 2012 ♦ Revision received 14 January 2013 ♦ Accepted 20 February 2013 ♦ Published online 4 April 2013

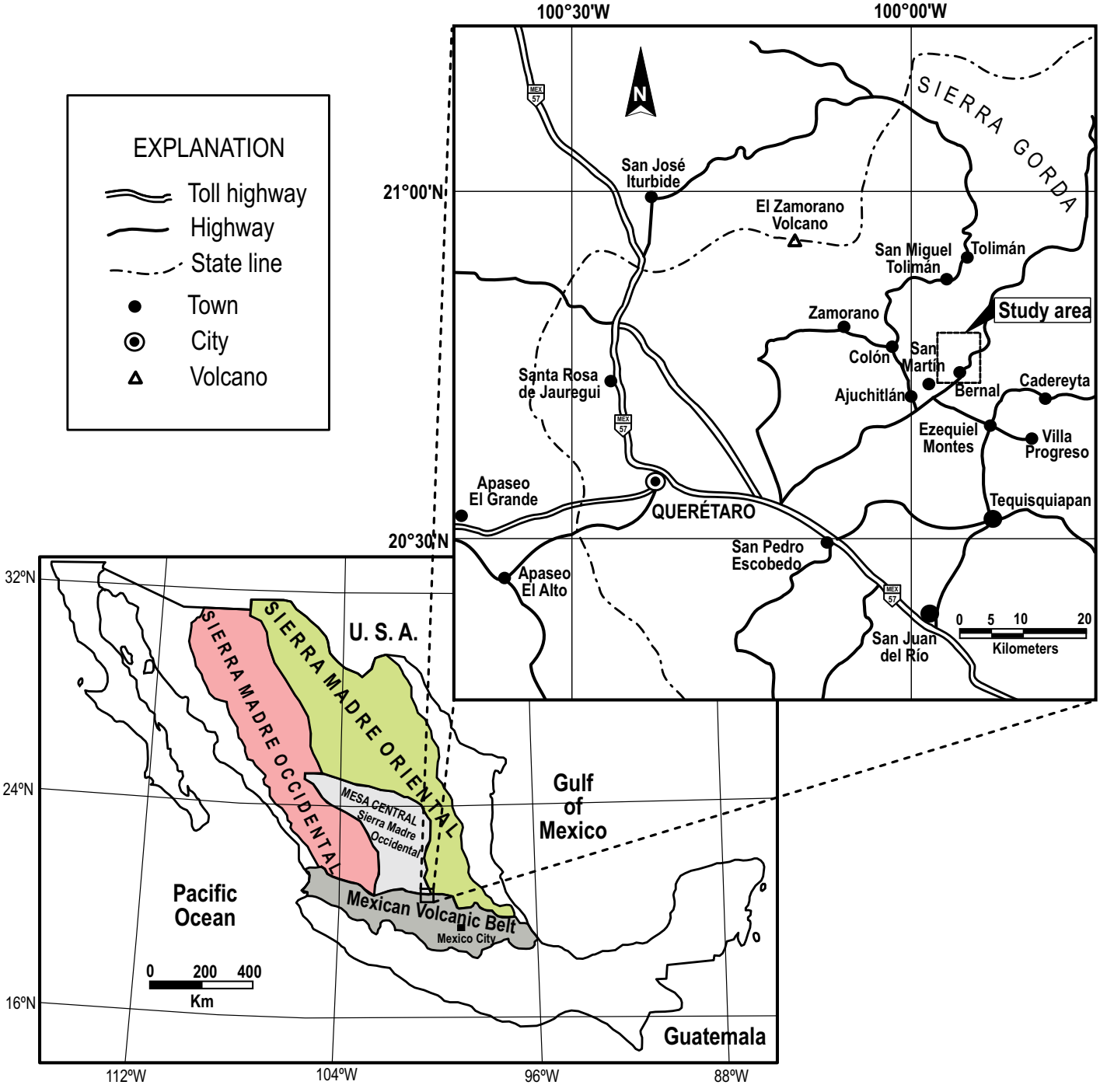

Figure 1. Index map showing the position of Peña de Bernal with respect to some of the geological provinces of Mexico and the geography of the local area; the study area is highlighted in the inset.

Las Trancas Formation (Jt)

Las Trancas Formation was defined by Segerstrom (1961) as a Jurassic–Early Cretaceous (Kimmeridgian–Barremian) marine sedimentary sequence. It consists of dark-gray fissile shales, calcareous limonites, and dirty limestones with pyrite and minor amounts of graywackes and flint (Segerstrom, 1961, 1962; Chauve et al., 1985; Carrillo-Martínez, 1990). In the Bernal area, this unit occurs as a thinly bedded sequence of fissile shales and limestones with minor amounts of graywackes. Bedding is generally undulated, with thicknesses in the order of tens of meters. The shales and limestones of Las Trancas Formation were intensively deformed during the Cretaceous–Tertiary (K-T) Laramide orogeny (Chauve et al., 1985;

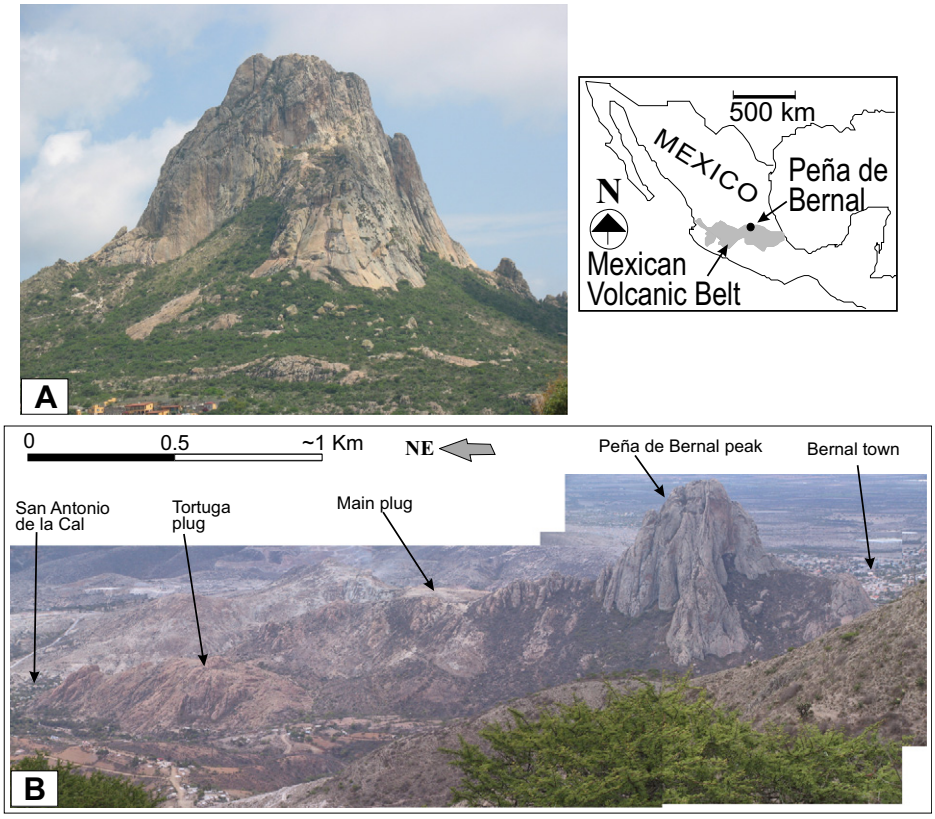

Figure 2. (A) Panoramic view toward the north of Peña de Bernal monolith and corresponding regional index map (inset). (B) Panoramic view toward the east of Peña de Bernal from summit of San Martín volcano. Note the elongated shape of the main plug of the Peña de Bernal dacitic dome and the rounded plug of Tortuga. The Northern plug is not shown in the image.

Padilla-y-Sánchez, 1985), producing incompetent folding, eastward thrust transportation, and a low-grade regional metamorphism (Suter, 1987; Carrillo-Martínez and Suter, 1990; Carrillo-Martínez, 1998; Bartolini et al., 1999) that gave a fissile and slate character to the shales and limestones, but without reaching the point of the schist facies.

El Doctor Formation (Kd)

El Doctor Formation is a middle Cretaceous (Albian–Cenomanian) unit that was defined by Wilson et al. (1955) from a locality near the town of El Doctor, in the Sierra Gorda portion of the Sierra Madre Oriental fold-thrust belt, and ~35 km to the NE of Bernal (Fig. 1). This formation is characterized by its origin as a reef and, thus, is composed mainly of platform calcareous small fossils and microfossils. In the mapped area, El Doctor Formation crops out to the NW of San Antonio de la Cal (Fig. 4), as an elongated outcrop between Las Trancas and Soyatal formations. The outcrop is ~100 m thick and consists mostly of gray fossiliferous limestones in thick to medium thick banks.

Soyatal Formation (Ks)

Soyatal Formation is a Late Cretaceous (Turonian) marine sedimentary sequence composed mainly of limestones and flint lenses (White, 1948). Index fossils near Bernal and found by us include ammonites of *Nowakites sp.* at the locality of Dedhó, and *Texamites sp.* in the Tolimán canyon, confirming the Late Cretaceous epoch of this unit. Soyatal Formation is thinly to medium bedded, showing boudinage primary bedding. It is dark gray when fresh, and light gray to white when weathered. As in Las Trancas, this unit was folded and northeastwardly tectonically transported during the K-T Laramide orogeny (Chauve et al., 1985). Las Trancas Formation was thrusted on Soyatal Formation during this orogeny (Suter, 1987; Carrillo-Martínez, 1998), forming klippes at top of younger Soyatal. In the Bernal area, the top of Soyatal Formation is eroded, and thus, a complete thickness estimate was not possible, but a minimum of 300 m is considered our best approach.

Lower Tertiary Continental Clastic Sediments (Ts)

Continental detrital deposits crop out to the NW of the mapped area and nearby the town of San Martín (Fig. 1). Within the mapped area these deposits occur as small patches in the SW lower flank of Peña de Bernal too small to be shown in Figure 4, and to the southwest of Cerro Azul, in the northeastern portion of the area. Thickness ranges from 0 to 20 m. Near Bernal this unit consists mainly of conglomerates with clast sizes of 2–30 cm in diameter, mainly from shales of Las Trancas Formation and black flint and limestones of Soyatal Formation. Clasts are rounded to semi-rounded and are supported by a red clay matrix, in parts weathered to a calcareous soil. The deposits at Cerro Azul are finer and consist of cross-bedded sandstones, green and red, with no base exposed, and covered by younger pyroclastic rocks. These clastic deposits rest unconformably either on Soyatal or Las Trancas formations. Tentatively, we position this unit in the lower Tertiary, after the K-T orogeny, in correlation with similar continental deposits of central Mexico, such as the Eocene red conglomerates of Guanajuato and Zacatecas (Edwards, 1955; Tristán-González et al., 2009), and the Cenicera formation of San Luis Potosí (Labarthe-Hernández et al., 1982).

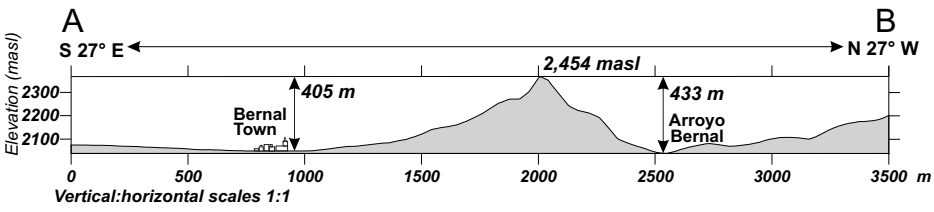

Figure 3. Topographic cross section outlining the height of Peña de Bernal. Map position of A–B section line is shown in Figure 4. masl—meters above sea level.

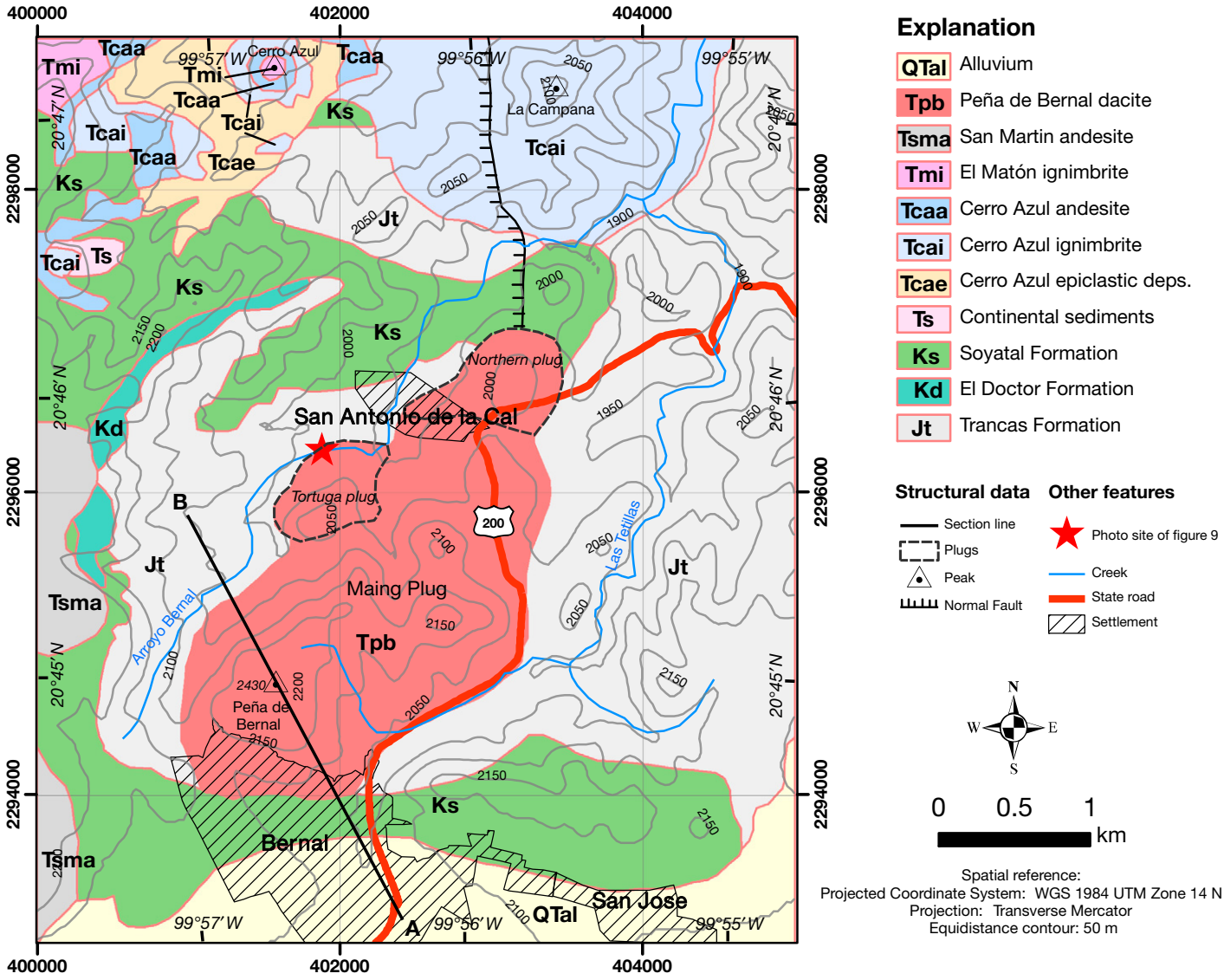

Figure 4. Geologic map of Peña de Bernal dacitic dome and surrounding area. Also indicated is the A–B section line shown in Figure 3.

Cerro Azul Epiclastic Deposits (Tcae)

Overlying the continental red bed deposits mentioned above, there is a sequence of epiclastic deposits consisting of green to yellow tuffaceous sands, in beds 20–100 cm thick, with cross bedding in places. Best exposures occur west of Cerro Azul, where the unit reaches up to 50 m in thickness (Fig. 4). The lower part of the sequence consists of beds of rounded to subangular clasts of quartz, plagioclase, and volcanic glass, supported by a clayey, chloritized matrix. The upper part is mainly a clay deposit, in beds of 2–20 cm. It is possible that these deposits, and particularly the upper clay beds, represent reworked basal ash deposits precursor to the emplacement of Cerro Azul ignimbrite, which conformably overlies this unit.

Cerro Azul Ignimbrite (Tcai)

Cerro Azul ignimbrite is a widespread, densely welded, orange-brown unit, with up to 30 vol% of phenocrysts (2–3 mm) of quartz, sanidine, and biotite, supported in a matrix of devitrified glass shards. The thickness at Cerro Azul is up to 45 m, but more commonly it is around 30 m thick. The base of the ignimbrite includes a pink unwelded to poorly welded ash layer, up to 1 m thick, that lacks bedding, phenocrysts, and/or lithics. Conformably and continuously overlying this basal layer is the massive part of the welded ignimbrite. Above the ash layer, the ignimbrite contains sparse lithics of limestone and chert. K-Ar age dating performed on this unit yielded an age of 31.5 ± 0.7 Ma (Table 1). Therefore, this ignimbrite corresponds to mid-Tertiary volcanism related to the Sierra Madre Occidental.

Cerro Azul Andesite (Tcaa)

Andesitic lavas overlie Cerro Azul ignimbrite (Fig. 5). These lavas have been informally named as Cerro Azul andesite because the best exposures are found at Cerro Azul and at hills to the west of it. The andesite lavas usually form plateaus and apparently were fed from fissures. Some andesitic dikes with similar aspect and texture were observed nearby cutting the Cerro Azul epiclastic deposits and the Cerro Azul ignimbrite. Whole-rock K-Ar dating of this unit resulted in 29.4 ± 0.8 Ma (Table 1). It is generally a propylitized gray to green rock or

dark gray, when rare fresh andesite is found. In some sites, it has vesicles or amygdules of agate or chalcedony. Andesite is fine grained, with sparse phenocrysts with sizes of less than 1 mm of plagioclase, Fe-Ti oxides, and clinopyroxene (augite), which sometimes is bordered by a rim of amphibole.

El Matón Ignimbrite (Tmi)

El Matón ignimbrite is one of the largest in distribution and volume of the region, and is commonly observed between Tolimán and San Miguel (outside the mapped area; Fig. 1). It is a partly welded, pink, rhyolitic ignimbrite, with eutaxitic texture. This is a crystal-rich ignimbrite, with up to 40 vol% of phenocrysts of quartz, sanidine, and oxidized biotite. Most crystals are subhedral and broken, with sizes between 1 and 3 mm. A matrix of devitrified glass shards is preserved. The degree of welding increases upward, from poorly to densely welded. It overlies Cerro Azul andesite, making the top of the hill with this name (Fig. 5). It also overlies Soyatal Formation and the lower Tertiary clastic sediments. K-Ar dating yields an age of 29.4 ± 0.7 Ma (Table 1). The ignimbrite is stratigraphically younger than 29.4 ± 0.8 Ma Cerro Azul andesite, although both resulted with the same isotopic age.

San Martín Andesite (Tsma)

San Martín andesite includes a series of lavas erupted from San Martín volcano that are between the towns of San Martín and Bernal (Fig. 1). A couple of small outcrops can be observed at the southwestern part of the mapped area (Fig. 4). San Martín andesite overlies Las Trancas and Soyatal formations, and El Matón ignimbrite outside the mapped area. The lavas are dark gray to light gray and generally form thick lobes rather than plateaus. Lavas are porphyritic, with up to 20 vol% of phenocrysts of plagioclase and hornblende and a groundmass made of glass and microlites of the same phases plus sparse olivine. The structure of the lavas includes flow banding and flow foliation. K-Ar dating of two different lava units of San Martín volcano yielded ages of 11.0 ± 0.3 Ma and 10.2 ± 0.2 Ma (Table 1), suggesting a long-lived polygenetic history of this volcano. San Martín volcano is similar in age and composition with other middle Miocene stratovolcanoes in the region, such as La Joya and El Zamorano, which are related to the Mexican Volcanic Belt (Aguirre-Díaz, 2008).

THE PEÑA DE BERNAL DACITIC DOME

Description

Peña de Bernal is a highly crystalline and very resistant rock, gray to light gray when fresh and brown when weathered. It is composed of up to 80 vol% crystals and 20 vol% matrix glass; phenocrysts make up to 30 vol% of the total. Mineralogy includes plagioclase + orthopyroxene + hornblende + biotite + sanidine + quartz + Fe-Ti oxides + apatite + zircon (Fig. 6). It has a porphyritic texture with phenocryst content varying within 15–30 vol%. Amongst phenocrysts, plagioclase and hornblende are the most common and largest up to <2.5 mm; biotite and pyroxene are smaller and relatively less abundant. Mafic phases are generally oxidized either completely or along their rims (Fig. 6). The matrix is made of a microcrystalline mineral assemblage with all the phases mentioned above, plus interstitial glass. Plagioclase phenocrysts are generally zoned with complex oscillatory zoning and fritted zones (Fig. 6). Sanidine is rare, but it has been observed as phenocrysts. Glass is pale brown and occurs between the crystals. Textures suggest a long-term, complex cooling history of the Peña de Bernal magma, with resorption of phases and disequilibrium and reequilibration conditions, particularly recorded in the plagioclase. The large mineral assemblage includes most phases of the Bowen's series (except olivine), suggesting enough time for the nucleation and growth of all these phases with the liquid line of descent (Wilcox, 1979).

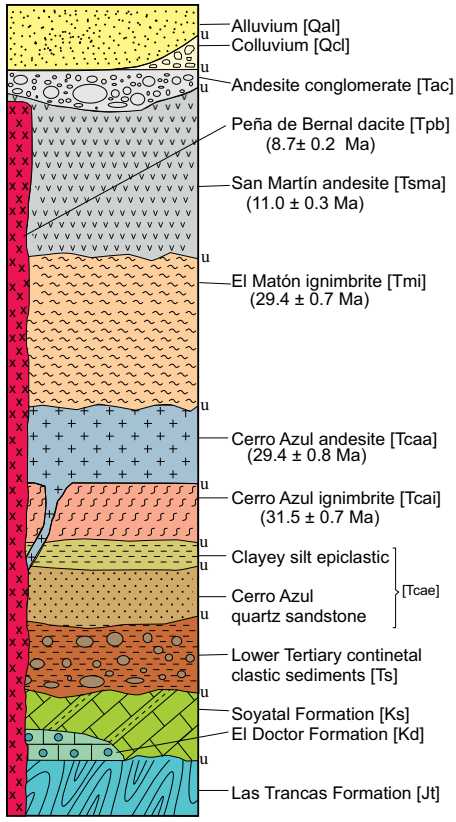

Figure 5. Composite stratigraphic column for the area shown in Figure 4. u—unconformity.

Age

Two samples of Peña de Bernal were analyzed to determine its age. Samples were processed in separate laboratories and using different techniques in order to cross-check the results and to

TABLE 1. K-Ar and ^{40}Ar-^{39}Ar ISOTOPIC AGES OF THE BERNAL AREA, QUERÉTARO

Unit*	Sample number	Coordinates Latitude N	Coordinates Longitude W	Age (±1σ)	^{40}Ar* (e-7 cc)	^{40}Ar* (%)	K_2O (wt%)	Fraction†	Analyzed weight (g)
Tpb	SM10-05	99°56.67′	20°45.58′	8.7 ± 0.2	7.24	71.4	2.13	GM	0.4759
Tpb	Qro-8$^{Ar/Ar}$	99°56.73′	20°44.71′	8.7 ± 0.2^{Tp}	4.52	60.5	—	PLG	0.6122
Tsma	SM09-05	99°59.04′	20°44.15′	10.2 ± 0.2	4.69	73.1	1.43	WR	0.5101
Tsma	SM03-05	99°58.39′	20°44.70′	11.0 ± 0.3	6.31	39.6	1.78	WR	0.6035
Tmi	SM14-05	99°57.16′	20°46.95′	29.4 ± 0.7	4.83	77.8	5.06	WR	0.5002
Tcaa	SM13-05	99°57.02′	20°47.02′	29.4 ± 0.8	11.5	49.8	1.21	WR	0.6223
Tica	SM12-05	99°56.76′	20°47.07′	31.5 ± 0.7	5.71	96.5	5.58	WR	0.5201

Units dated: Tpb—Peña Bernal dacite; Tsma—San Martín andesite; Tmi—El Matón ignimbrite; Tcaa—Cerro Azul andesite; Tica—Cerro Azul ignimbrite. All except Qro-8 are K-Ar ages done at Université de Bretagne Occidental, Brest, France, by Hervé Bellon (technique described in Bellon et al., 1981). ^{40}Ar-^{39}Ar analysis done at División de Ciencias de la Tierra, Centro de Investigación Científica y de Educación Superor de Ensenada (CICESE), Baja California, México, by Margarita López-Martínez (technique described in Cerca-Martínez et al., 2000); Tp plateau age calculated with more than 75% of ^{39}Ar released on four fractions. ^{40}Ar—extracted radiogenic ^{40}Ar in standard cubic cm (cc) and percent (%).
†Material used: WR—whole rock, GM—groundmass, PLG—plagioclase.

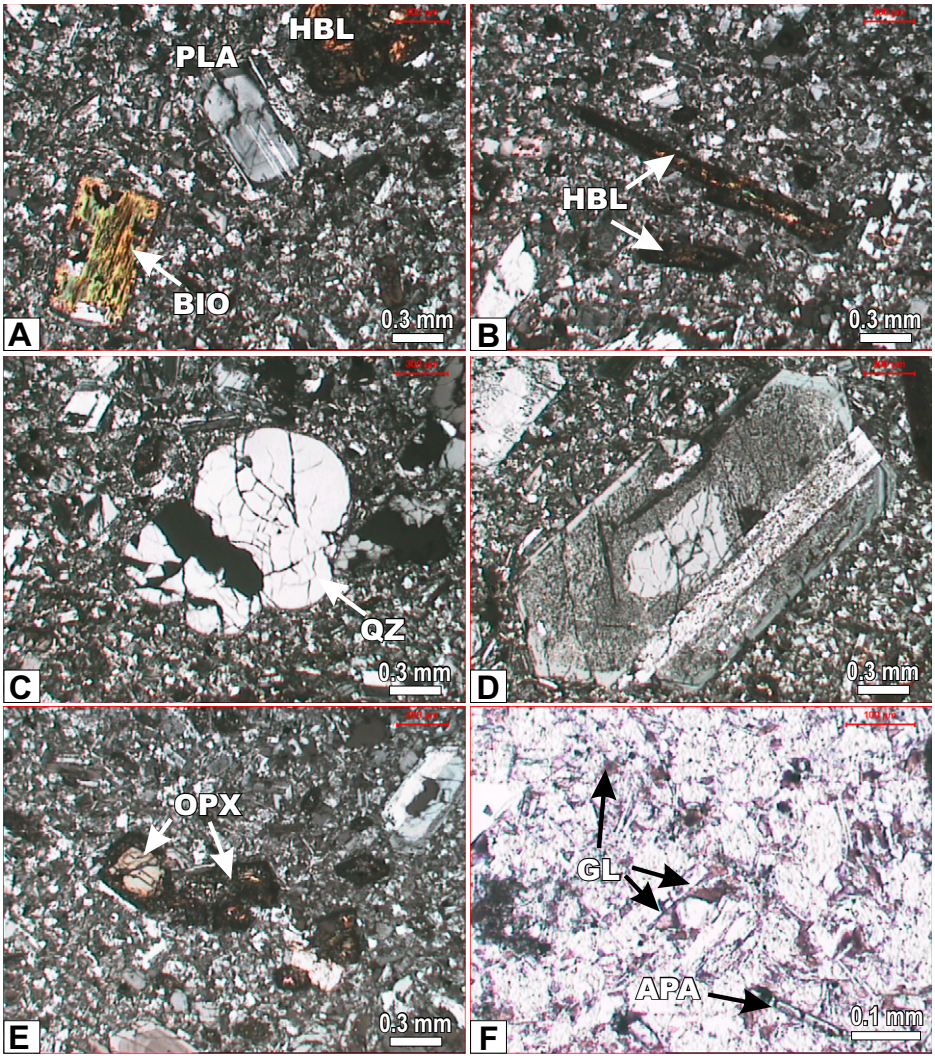

Figure 6. Representative photomicrographs of Peña de Bernal dacite, all with crossed polarizers (except F). (A) Phenocrysts of plagioclase (PLA), hornblende (HBL), and biotite (BIO) in a microcrystalline + glass matrix. (B) Large crystals of acicular hornblende (HBL) partly oxidized. (C) Phenocryst of rounded quartz (center). (D) Large phenocryst of plagioclase showing complex oscillatory zoning and fritted zones. (E) Euhedral crystals of orthopyroxene with oxidized rims. (F) Accessory apatite (APA) and glass patches between matrix crystals. Graphic scales in mm and microns indicated in each photograph.

have a good accuracy of the timing of formation. The K-Ar age obtained at the University of Brest, France, yielded 8.7 ± 0.2 Ma (Table 1). The ^{40}Ar-^{39}Ar plateau age obtained at the Centro de Investigación Científica y de Educación Superior de Ensenada (CICESE) research center in Ensenada, Mexico, yielded also 8.7 ± 0.2 Ma on plagioclase separate (Fig. 7 and Table 2). Therefore, 8.7 ± 0.2 Ma should be the age of Peña de Bernal dacite. The middle Miocene age of Peña de Bernal is consistent with the general age of other silicic domes in the central-northern sector of the Mexican Volcanic Belt (Aguirre-Díaz et al., 1998; Aguirre-Díaz, 2008).

Structure

Besides the main igneous mass that forms the peak of Peña de Bernal, there are two other plugs with lower elevations, and all three plugs crop out in a 4.8 km^2 area (Figs. 2 and 4). The main plug extends for ~3.5 km from the highest peak that forms Peña de Bernal to the southwesternmost part at San Antonio de la Cal (Fig. 4). The other two plugs are La Tortuga, 0.85 × 0.45 km, at the western portion of the main outcrop, and the Northern plug, at the northeasternmost part of the outcrop (Fig. 4). The rock is similar in all plugs with some textural or dome foliation variations; textures vary mainly in crystal size with crystals bigger in the main plug and smaller in the other two. Apparently, plugs were emplaced simultaneously, as there are not sharp contacts between them but rather transitional contacts. Peña de Bernal peak shows dome foliation that varies from ~40° inward dips at the margins to nearly vertical dips at the center of the dome (Fig. 8). This foliation follows the general elongated trend of the main plug to the NE. Peña de Bernal dacite is in intrusive contact with the country rock, which is primarily the Las Trancas Formation, although it is also in contact with the Soyatal limestone in some places, in particular along the southwestern margin of the outcrop area (Fig. 4). It is not a thermal metamorphic aureole caused by the dome intrusion, and contact metamorphism of the country rock is also not observed. The metamorphism of Las Trancas Formation was caused by a regional tectonic event (Suter, 1987) and not by the intrusion of Peña de Bernal dome. The contact between the Peña de Bernal dacite and the country rock is sharp (Fig. 9A). Most notable is the fact that it looks like a normal fault contact, with vertical slickensides marked in the country rock, in particular in Las Trancas Formation (Fig. 10). The Peña de Bernal dacite near the contact is fractured but not brecciated, forming fractures with a peculiar orthogonal arrangement (Fig. 10A). Also observed along the margin of Peña de Bernal dome are sheared marginal zones that form wavy trends in map view between Peña de Bernal and the country rock (Fig. 10B). These observations indicate a rigid (fragile) behavior of the Peña de Bernal dacite along its margins during intrusion, which is discussed below.

Chemistry

Two whole-rock analyses of the Peña de Bernal rock yielded a dacitic composition following the total-alkalis (TAS) classification of Le Bas et al. (1986) (Fig. 11A). Whole-rock analyses resulted in SiO_2 = 67 wt% and Na_2O + K_2O = 6 wt% (normalized volatile-free, Table 3), which are plotted in the corresponding TAS diagram, together with other volcanic units of the mapped area, such as the Oligocene rhyolitic ignimbrites and the Miocene San Martín andesite (Fig. 11A). For comparison, analyses for other units from the region are plotted too, such as the Miocene andesite of El Zamorano volcano and a Pliocene basaltic andesite from the Cenizas locality, both reported by Aguirre-Díaz and López-Martínez (2001).

Cerro Azul ignimbrite chemistry resulted in SiO_2 = 72.5%, Al_2O_3 = 11.7%, Na_2O = 1.3%, K_2O = 5.35%, with a high value for loss of ignition (LOI) of 4% (Table 3), probably because

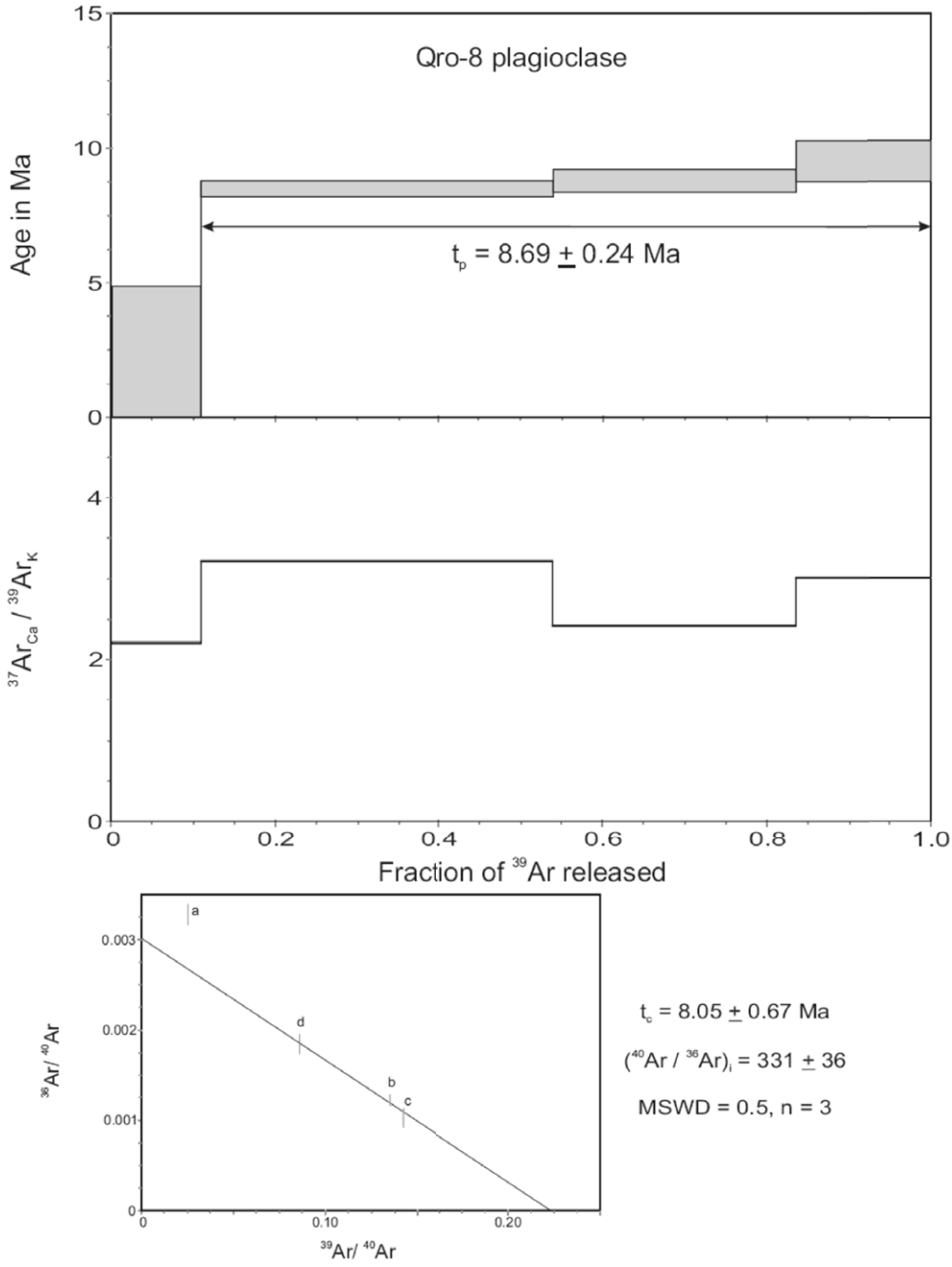

Figure 7. ^{40}Ar/^{39}Ar age spectra of Peña de Bernal dacite (sample Qro-8, Tables 1 and 2).

TABLE 2. ^{40}Ar-^{39}Ar DATA OF SAMPLE QRO-8 PLAGIOCLASE

Temp. (°C)	F ^{39}Ar	^{40}Ar*/^{39}Ar$_K$	1σ	t (Ma)	1σ		^{40}Ar* (%)	^{40}Ar/^{36}Ar	^{37}Ar$_{Ca}$/^{39}Ar$_K$	t_i (Ma)	t_p (Ma)	t_c (Ma)	(^{40}Ar/^{36}Ar)$_i$	MSWD/n
800	0.1092	0.51	0.64	2.16	2.71	†	3.04	304.78	2.21					
1000	0.4304	2.00	0.07	8.50	0.30	§	63.77	815.71	3.22					
1300	0.2955	2.07	0.10	8.79	0.42	§	69.52	969.39	2.42					
1500	0.1650	2.25	0.18	9.52	0.76	§	45.39	541.08	3.02	8.06 ± 0.41	**8.69 ± 0.24**	8.05 ± 0.67	331 ± 36	0.5/3

Note: Experiments were conducted with a MS-10 mass spectrometer on-line with a Modifications Ltd. Ta-furnace; 0.6122 g of plagioclase concentrate were used for the step-heating experiment. Temp. °C is the temperature used to release argon; t is the age of the individual fraction (it does not include the uncertainty in J); t_i—integrated age; t_p—plateau age calculated with the weighted mean of the fractions identified with the symbol §; t_c—isochron age calculated ignoring the fraction identified with the symbol †; MSWD/n is the goodness of fit and number of points used to calculate the isochron age; all errors are given to 1σ level. J—0.002356 ± 0.000016. Preferred age is highlighted in bold typeface. MSWD—mean square of weighted deviates. To calculate the ^{40}Ar-^{39}Ar ages, the constants recommended by Steiger and Jäeger (1977) were used. The equations presented in York et al. (2004) were used in all the straight line calculations. The internal standard used as irradiation monitor was calibrated with international standards, using the ages given in Renne et al. (1998).

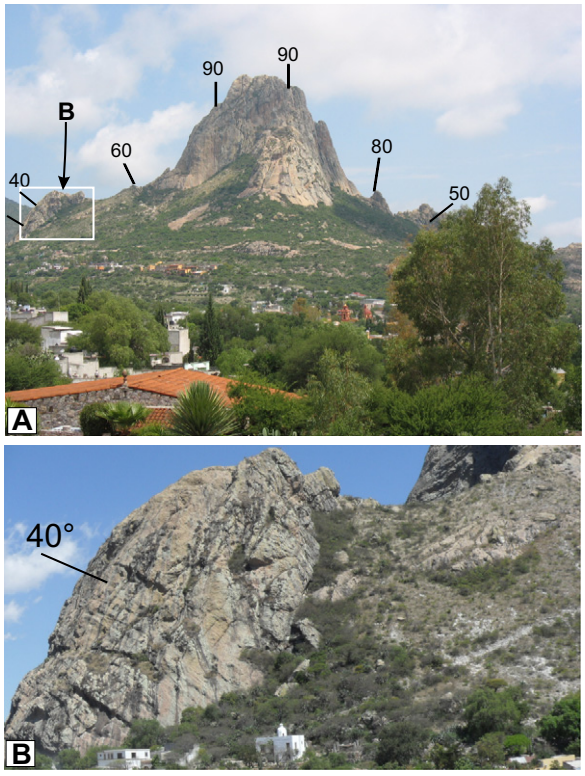

Figure 8. (A) Dome foliation of Peña de Bernal in a view to the N, foliation dips from ~40° at borders to vertical in the central zone. (B) Detail of inward-dipping foliation on the western flank in a close-up of the area shown within white frame.

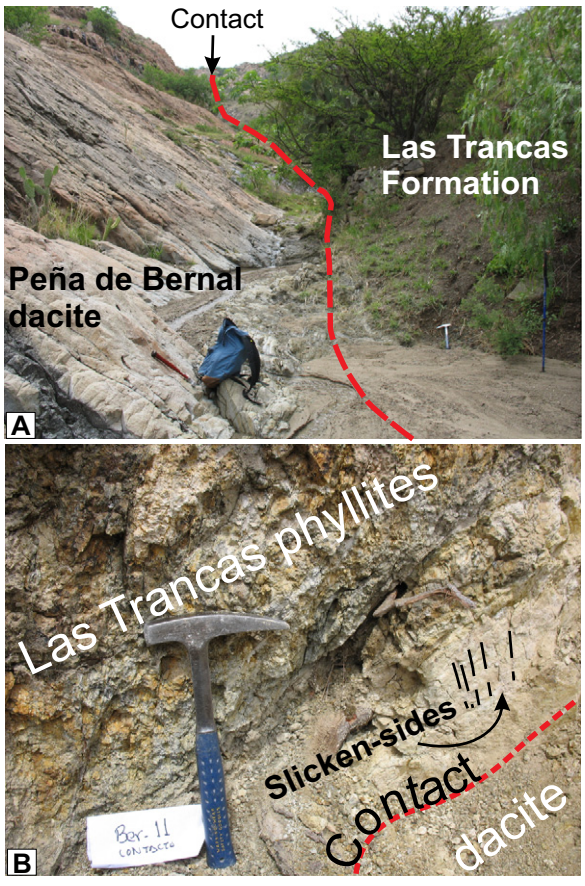

Figure 9. (A) Contact between Peña de Bernal dacite and Las Trancas Formation. Cooling joints of dacite shown in photograph are perpendicular to the dome foliation (not evident in photograph), which dips inward. (B) Vertical slickensides at sheared contact surface on Las Trancas Formation (slightly metamorphosed shales due to regional metamorphism). Location of site in photographs is showing in Figure 4.

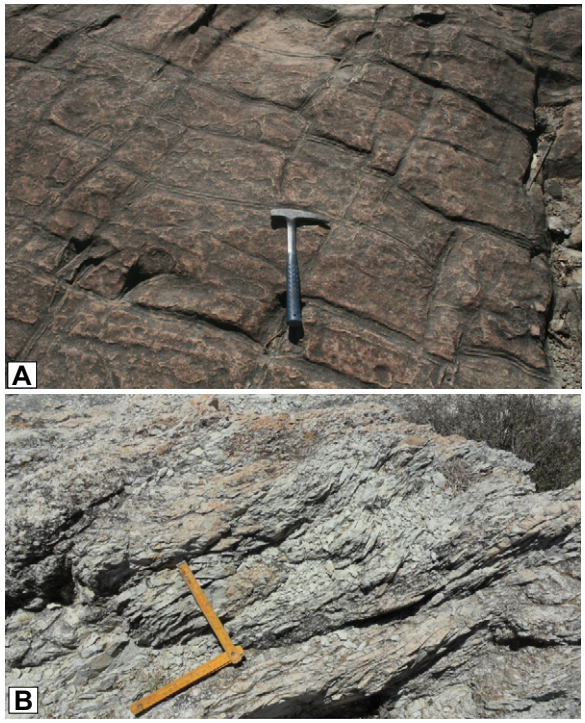

Figure 10. (A) Orthogonal fracturing observed along the inner margin of Peña de Bernal dome, near the intrusive contact with the country rock. Peña de Bernal dacite at its margin is fractured but not brecciated. (B) Plane view of the intensively sheared border zone of Peña de Bernal dacite next to the contact with the country rock caused by forceful intrusion (ruler for scale is 20 × 20 cm).

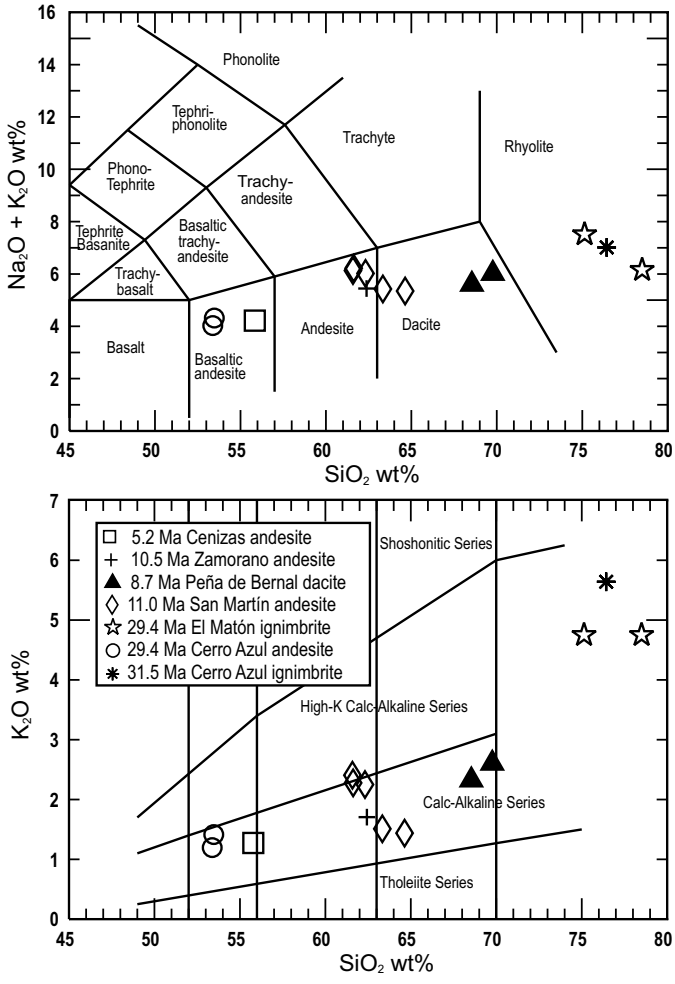

Figure 11. (A) Total alkalis-silica (TAS) plot of Le Bas et al. (1986) of analyzed samples of the Peña de Bernal area and neighboring volcanic rocks reported by Aguirre-Díaz and López-Martínez (2001). (B) SiO_2 versus K_2O plot of same samples shown in (A) with classification of Peccerillo and Taylor (1976).

TABLE 3. MAJOR-ELEMENT CHEMISTRY ON WHOLE-ROCK SAMPLES OF THE BERNAL AREA, QUERÉTARO

Sample	SM12-05	SM11-05	SM13-05	SM02-05	SM14-05	SM03-05	SM04-05	SM05-05	SM06-05	SM08-05	Qro-32	SM10-05	Qro-8	Qro-4
Unit	Tcai	Tcaa	Tcaa	Tmi	Tmi	Tsma	Tsma	Tsma	Tsma	Tsma	Tza	Tpb	Tpb	Tca
Rock type	R	BA	BA	R	R	A	D	A	D	A	A	D	D	BA
Major elements														
SiO_2	72.500	51.800	51.300	73.400	73.900	60.600	62.500	60.400	62.500	61.500	62.00	67.600	67.03	54.92
TiO_2	0.130	1.960	1.850	0.140	0.080	0.990	0.840	1.000	0.710	1.000	0.97	0.400	0.46	2.07
Al_2O_3	11.760	15.220	15.200	13.850	11.800	16.150	17.000	15.600	17.350	16.100	17.61	15.400	16.39	16.85
Fe_2O_3T	2.410	10.420	10.390	2.050	1.350	5.320	4.750	5.380	4.640	5.160	5.36	2.850	3.02	9.25
MnO	0.030	0.180	0.160	0.020	0.020	0.080	0.080	0.080	0.040	0.070	0.09	0.050	0.05	0.14
MgO	0.740	5.070	5.750	0.150	0.690	2.610	2.230	2.740	0.990	2.390	2.54	1.390	1.32	3.71
CaO	0.700	8.120	7.680	0.820	0.550	6.300	5.890	6.720	5.280	6.320	5.66	3.420	4.07	7.48
Na_2O	1.300	2.810	2.720	2.700	1.320	3.870	3.860	3.650	3.780	3.720	3.70	3.300	3.20	2.87
K_2O	5.350	1.370	1.150	4.640	4.470	2.240	1.490	2.360	1.390	2.220	1.71	2.520	2.27	1.23
P_2O_5	0.060	0.600	0.580	0.020	0.020	0.470	0.310	0.450	0.280	0.500	0.28	0.120	0.13	0.33
LOI	4.220	2.580	3.240	1.980	5.040	0.690	0.900	1.290	2.600	1.100	0.58	2.870	1.75	0.32
Total	99.200	100.130	100.010	99.770	99.240	99.320	99.850	99.670	99.640	100.080	100.50	99.920	99.72	99.16
Major elements (free volatiles calculated with the SINCLAS program; Verma et al., 2002)														
SiO_2	76.430	53.470	53.382	75.136	78.508	61.631	63.339	61.587	64.639	62.318	62.243	69.766	68.545	55.888
TiO_2	0.137	2.023	1.925	0.143	0.085	1.007	0.851	1.020	0.734	1.013	0.974	0.413	0.478	2.106
Al_2O_3	12.397	15.711	15.817	14.177	12.536	16.425	17.228	15.906	17.944	16.314	17.679	15.894	16.76	17.147
Fe_2O_3	1.256	3.818	3.744	1.077	0.69	2.342	2.042	2.358	2.017	2.263	2.279	1.340	1.376	3.446
FeO	1.156	6.242	6.359	0.919	0.669	2.761	2.494	2.814	2.503	2.668	2.792	1.441	1.540	5.370
MnO	0.032	0.186	0.166	0.020	0.021	0.081	0.081	0.082	0.041	0.071	0.091	0.052	0.055	0.146
MgO	0.780	5.233	5.983	0.154	0.733	2.654	2.260	2.794	1.024	2.422	2.550	1.434	1.354	3.775
CaO	0.738	8.382	7.992	0.839	0.584	6.407	5.969	6.852	5.461	6.404	5.682	3.530	4.162	7.612
Na_2O	1.370	2.900	2.830	2.764	1.402	3.936	3.912	3.722	3.909	3.770	3.714	3.406	3.272	2.921
K_2O	5.640	1.414	1.197	4.750	4.749	2.278	1.510	2.406	1.438	2.250	1.717	2.601	2.321	1.252
P_2O_5	0.063	0.619	0.604	0.020	0.021	0.478	0.314	0.459	0.290	0.507	0.279	0.124	0.134	0.337
CIPW normative minerals (calculated with the SINCLAS program; Verma et al., 2002)														
Q	43.891	7.317	7.294	38.636	49.639	14.722	19.341	14.872	23.171	16.820	18.057	30.214	29.614	12.590
Or	33.330	8.356	7.074	28.071	28.065	13.462	8.924	14.218	8.498	13.297	10.147	15.371	13.716	7.399
Ab	11.592	24.539	23.946	23.388	11.863	33.305	33.102	31.494	33.077	31.900	31.427	28.82	27.687	24.716
An	3.250	25.675	26.919	4.032	2.760	20.421	24.988	19.587	25.198	20.946	26.366	16.703	19.773	29.977
C	2.847	—	5.328	3.011	4.078	—	—	—	0.722	—	0.047	1.354	1.618	—
Di	—	9.554	7.062	—	—	6.562	2.056	9.081	—	5.983	—	—	—	4.497
Hy	2.861	13.745	17.219	0.983	2.383	5.111	6.285	4.328	4.343	4.675	8.155	4.525	4.376	11.044
Ol	—	5.535	—	1.561	—	3.395	2.96	3.418	2.924	—	—	—	—	—
Mt	1.821	—	5.428	—	1.000	—	—	—	—	3.281	3.304	1.943	1.995	4.996
Hm	—	3.842	—	0.272	—	1.912	1.616	1.937	1.394	—	—	—	—	—
Il	0.260	1.434	3.656	0.046	0.161	1.107	0.728	1.063	0.672	1.924	1.850	0.784	0.908	4.000
Ap	0.146	0.003	1.399	0.023	0.049	0.007	0.003	0.005	0.005	1.175	0.640	0.287	0.310	0.781

Note: Rock type refers to the chemical classification according to total-alkalis versus silica diagram (Le Bas et al., 1986); Fe_2O_3T-Fe_2O_3 as total iron; BA—basaltic-andesite; A—andesite; R—rhyolite; D—dacite. Unit refers to the lithostratigraphic unit according to the geological map and stratigraphic column shown in Figures 4 and 5. Tcai—Cerro Azul ignimbrite, Tcaa—Cerro Azul andesite, Tmi—El Matón ignimbrite, Tsma—San Martín andesite, Tza—Zamorano andesite, Tca—Cenizas andesite, Tpb—Peña de Bernal dacite. Qro-4 and Qro-32 are samples reported by Aguirre-Díaz and López-Martínez (2001); these two and sample Qro-8 were analyzed at the laboratory of Instituto de Geología at Universidad Nacional Autónoma de México (UNAM) using X-ray diffraction technique (Lozano-Santacruz and Bernal, 2005). The series SM samples were analyzed at the University of Brest, France, using inductively coupled plasma–atomic emission spectroscopy (Cotten et al., 1995).

we analyzed partly devitrified pumice fragments, indicating a rhyolitic composition in the TAS diagram (Fig. 11A). Major-element chemistry of Cerro Azul andesite yielded SiO_2 = 58.0%, Al_2O_3 = 15%, TiO_2 = 0.82%, Fe_2O_3 = 4.6%, Na_2O = 2%, and K_2O = 1.37% (Table 3), corresponding to a basaltic andesite composition in the TAS classification. Chemical analyses of El Matón ignimbrite yielded SiO_2 ~73%, Al_2O_3 = 11%–13%, Na_2O = 1.3%–2.7%, and K_2O ~4.4%. It classifies as rhyolite in the TAS diagram (Fig. 11A). However, it should be noted that the analyzed pumice was devitrified. Chemical data of two analyzed samples from San Martín andesite show SiO_2 = 60.4%–64.9%, Al_2O_3 = 15.4%–17.0%, TiO_2 = 0.4%–1.0%, Fe_2O_3 = 2.8%–5.3%, Na_2O ~3.6%, and K_2O = 1.3%–2.5% (Table 3). These values result in a TAS classification of andesite to dacite (Fig. 11A).

Peña de Bernal dacite as well as other volcanic units sampled from the Bernal area all are calc-alkaline, low-K silicic rocks, as shown in the SiO_2-K_2O plot with the classification of Peccerillo and Taylor (1976; Fig. 11B). According to these results, the suite of Oligocene, Miocene, and Pliocene rocks, and in particular the Peña de Bernal dacite, corresponds to a continental margin subduction zone setting (Wilson, 1989). This tectonic setting agrees well with the fact that the Peña de Bernal lies within the Mexican Volcanic Belt, which has been described as a volcanic province formed during a continental margin subduction zone tectonic regime (Aguirre-Díaz et al., 1998; Siebe et al., 2006).

Peña de Bernal dacite is relatively poorer in silica and alkali content with respect to other volcanic rocks in the area, such as the rhyolitic ignimbrites of El Matón and Cerro Azul. On the other hand, it is relatively more evolved than the neighboring andesites, such as those erupted from the San Martín volcano and the Cenizas andesite in the Amazcala caldera area (Fig. 12). This may be explained by the crystal-rich content of Bernal dacite (up to 80 vol%) with respect to these rhyolites, because crystals and in particular plagioclase tend to lower the silica and NaO_2 + K_2O contents in the whole-rock composition. The glass composition described below confirms this point.

Microprobe analyses of glass show a higher Na_2O + K_2O content than the whole-rock composition, yielding a trachytic composition of SiO_2 = 65 wt% and Na_2O + K_2O = 13 wt% (Table 4; Fig. 13). Mineral chemistry (Table 5) indicates a wide range in plagioclase composition from An_{20} to An_{60} (Fig. 14). This range is confirmed in textures observed in large plagioclases with oscillatory zoning and fritted cores

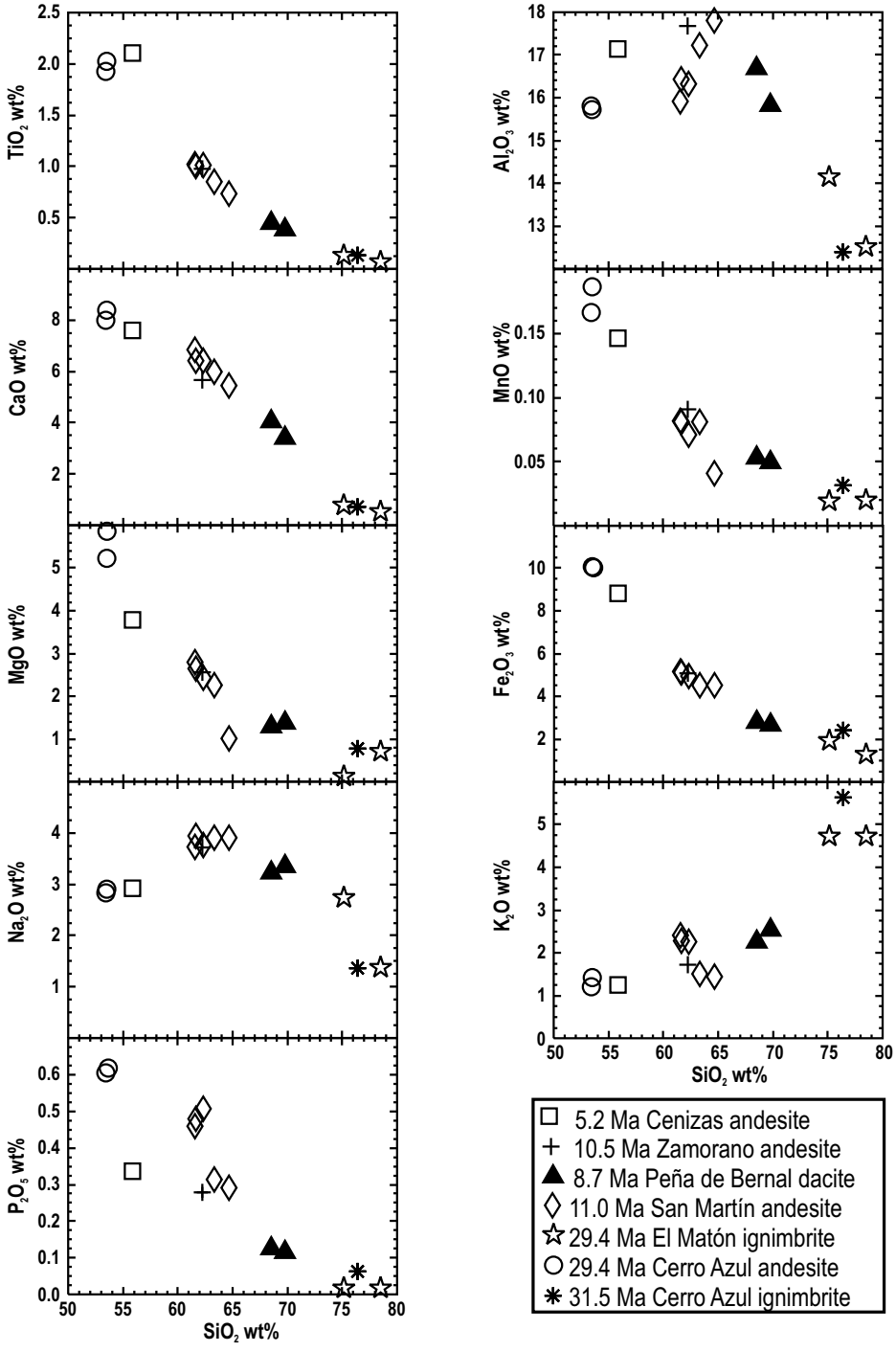

Figure 12. Harker plots (silica versus X component) of volcanic rocks of the Peña de Bernal area and vicinity (Cenizas and El Zamorano andesites).

(Fig. 6D). They generally have Ca-rich cores and Na-rich margins, suggesting a crystallization that followed the liquid line of descent of the Bowen's series (Wilcox, 1979). Two microprobe analyses confirm that orthopyroxene compositions correspond to enstatite (Fig. 14). Energy dispersive spectroscopy (EDS) analyses (not shown in Table 5) confirm the presence of biotite and hornblende and of the accessory phases, apatite and zircon.

Oxygen fugacity and corresponding equilibration temperatures were calculated based upon microprobe analyses on Fe-Ti oxides and pyroxene (Table 5). The temperature and

TABLE 4. GLASS CHEMISTRY OF PEÑA DE BERNAL DACITE

Sample	Qro-8A	Qro-8B	Qro-8C
SiO_2	65.41	65.49	64.88
TiO_2	—	—	—
Al_2O_3	18.82	19.41	19.07
FeO	0.02	0.06	0.20
MnO	—	—	—
MgO	—	—	—
CaO	0.38	0.45	0.43
Na_2O	3.59	4.61	3.51
K_2O	10.06	8.23	10.10
Cr_2O_3	0.01	—	—
BaO	1.73	1.74	1.80
Total	100.01	100.00	100.00

Note: Glass analyses by scanning electron microprobe using a Jeol-100 at the Paris 6 University-Jussieau Place performed by G. Aguirre-Díaz.

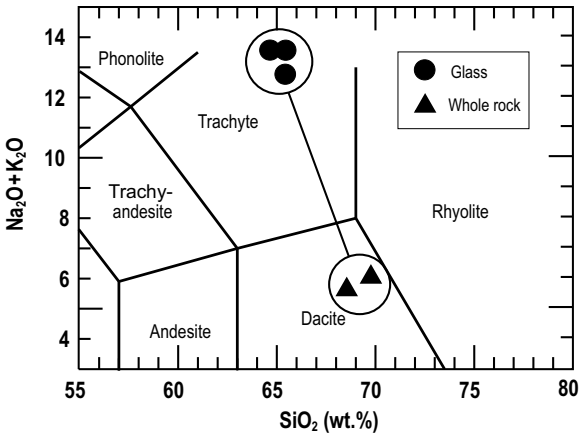

Figure 13. Total alkalis-silica (TAS) plot of Le Bas et al. (1986) of glass analyses obtained with the microprobe from samples of Peña de Bernal dacite.

oxygen fugacity (T-fO_2) parameters were calculated using the quartz-ilmenite-fayalite system proposed by Lindsley and Frost (1992) and the computer program QUILF (Andersen et al., 1993). Plotting the Peña de Bernal dacite data in a T-fO_2 diagram together with several buffers, a range of values is observed from T °C = 711.5, log fO_2 = –15.53 to T °C = 377, log fO_2 = –27.70, with several intermediate values (Fig. 15 and Table 6). The results plot between the nickel-nickel-oxide (NNO) and the hematite-magnetite (HM) buffers, indicating relatively high fO_2 conditions, which are common in subduction zone settings.

DISCUSSION

The Peña de Bernal area includes rocks of three major geologic provinces of Mexico: the Mesozoic Sierra Madre Oriental fold-thrust belt, the mid-Tertiary Sierra Madre Occidental volcanic province, and the Neogene–Quaternary Mexican Volcanic Belt. Focusing on the volcanic rocks, these include 31.5–29.4 Ma ignimbrites, 29.4 Ma andesites, 11–10 Ma andesites, and the 8.7 Ma Peña de Bernal dacite, which represents the youngest volcanic event in the mapped area (Fig. 4 and Table 1). The Oligocene ignimbrites and andesites crop out to the north of Peña de Bernal. At the base of this sequence is a layered succession of reworked pyroclastic deposits that in turn overlies continental red or green sandstones. The lower layered sequence resembles

TABLE 5. MINERAL CHEMISTRY FOR PEÑA DE BERNAL SAMPLES

Sample	1	2	3	4	5	6	7	8	9	10	11	12	13	14	15	16	17
SiO_2	50.90	51.83	52.97	53.54	56.27	56.16	53.88	57.63	58.22	61.94	61.89	61.77	56.51	60.31	54.44	54.08	54.17
TiO_2	0.09	0.03	0.09	0.07	—	—	0.16	0.05	—	—	—	—	0.12	0.03	0.04	0.10	0.06
Al_2O_3	30.29	29.98	28.75	28.82	27.03	27.27	28.20	26.10	25.31	23.16	22.54	22.90	26.60	24.78	28.22	28.00	28.00
FeO	0.35	0.23	0.36	0.18	0.29	0.38	0.41	0.29	0.32	0.35	0.39	0.32	0.02	0.04	0.41	0.20	0.33
MnO	—	0.15	—	0.09	0.05	0.02	0.02	0.06	—	—	0.01	—	—	—	—	—	0.01
MgO	0.06	0.06	—	0.04	—	—	0.03	0.04	0.03	—	—	—	—	0.00	0.03	0.01	—
CaO	13.40	12.37	11.62	11.15	9.50	9.16	10.04	8.01	5.90	4.14	4.64	4.31	8.71	6.39	10.74	10.76	10.76
Na_2O	3.91	4.61	4.91	5.24	5.83	6.04	5.69	6.81	7.54	8.90	8.41	8.18	6.70	7.39	5.50	5.62	5.65
K_2O	0.09	0.17	0.21	0.23	0.34	0.33	0.29	0.39	0.46	0.88	0.78	0.98	0.18	0.63	0.19	0.22	0.20
Cr_2O_3	—	0.02	0.10	—	0.03	0.04	0.03	0.04	—	—	0.12	—	0.09	—	—	0.11	0.02
Total	99.09	99.45	99.01	99.36	99.34	99.40	98.75	99.42	97.78	99.37	98.78	98.46	98.93	99.57	99.57	99.10	99.20

Sample	18	19	20	21	22	23	24	25	26	27	28	29	30	31	32	33	34
SiO_2	53.36	53.74	54.42	53.53	55.99	56.08	55.86	53.90	54.56	53.88	55.80	55.97	55.49	53.93	55.53	51.96	51.36
TiO_2	0.07	—	---	0.05	0.06	0.11	—	0.02	—	0.05	0.05	—	—	0.08	0.09	0.26	0.21
Al_2O_3	28.64	28.48	27.98	28.14	26.97	27.31	27.49	28.01	27.89	28.36	26.97	27.21	27.64	27.93	27.10	1.06	0.75
FeO	0.28	0.34	0.10	0.05	0.31	0.18	0.22	0.21	0.30	0.32	0.33	0.18	0.35	0.27	0.16	23.05	23.57
MnO	—	—	---	0.08	—	0.03	0.01	—	0.04	—	0.05	0.05	—	—	0.05	0.81	0.90
MgO	—	0.01	0.05	—	0.02	—	0.01	—	—	—	0.04	—	—	0.01	0.02	21.66	21.49
CaO	10.54	10.80	10.31	10.24	8.99	9.19	9.64	10.08	10.14	9.94	9.27	9.96	10.00	10.07	9.52	0.27	0.33
Na_2O	5.49	5.67	6.02	5.48	6.42	6.10	6.02	5.55	5.58	5.48	6.52	5.76	5.58	5.62	6.32	—	—
K_2O	0.17	0.20	0.20	0.29	0.41	0.26	0.33	0.22	0.29	0.28	0.40	0.28	0.33	0.30	0.42	—	—
Cr_2O_3	—	—	---	—	0.02	—	0.05	---	—	0.10	0.05	—	—	0.10	—	0.04	0.12
Total	98.55	99.24	99.08	97.86	99.19	99.26	99.63	97.99	98.80	98.41	99.48	99.41	99.39	98.31	99.21	99.11	98.73

Sample	35	36	37	38	39	40	41	42	43	44
SiO_2	—	0.01	0.01	0.07	0.05	0.46	—	0.30	0.16	0.05
TiO_2	47.35	45.80	45.58	6.37	0.93	1.64	0.88	7.25	0.43	0.91
Al_2O_3	0.04	0.07	0.07	4.24	0.78	1.12	1.13	2.12	0.82	0.75
FeO	48.44	46.71	42.73	79.33	91.30	86.72	89.00	79.63	90.86	90.09
MnO	0.96	1.22	2.35	0.27	—	0.07	0.09	0.64	0.11	0.11
MgO	1.32	1.55	2.00	0.98	0.23	0.24	0.30	0.63	0.30	0.16
CaO	0.02	0.65	0.09	0.03	0.01	0.09	0.05	0.05	0.04	0.05
Na_2O	0.01	—	0.02	0.05	—	—	—	0.08	0.03	—
K_2O	—	—	—	0.04	0.05	—	—	—	—	0.01
Cr_2O_3	0.06	0.02	0.01	0.12	0.03	—	0.03	—	—	—
Total	98.20	96.03	92.86	91.50	93.38	90.34	91.48	90.70	92.75	92.13

Note: Samples 1 to 32 are feldspar analyses, 33 and 34 are pyroxene analyses, and 35 to 44 are Fe-Ti oxides analyses. Microprobe analyses performed at Paris 6 University-Jussieau Place by Gerardo Aguirre-Díaz.

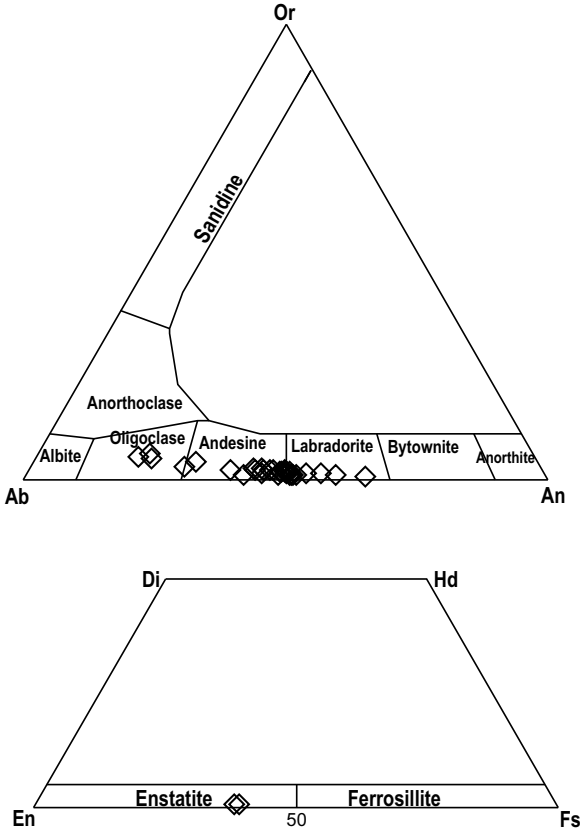

Figure 14. (A) Ternary plot showing feldspar composition and classification from microprobe analyses of plagioclases of Peña de Bernal dacite. (B) Quaternary plot of two pyroxene analyses and classification.

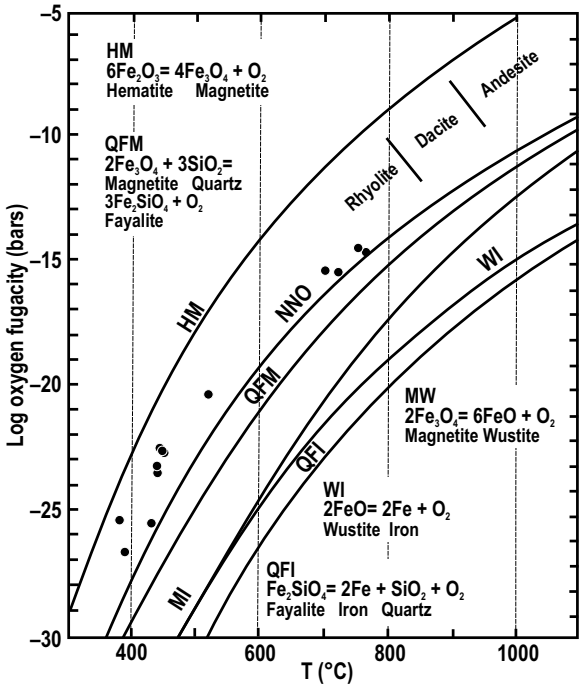

Figure 15. Temperature versus oxygen fugacity plot of Peña de Bernal dacite, obtained from Fe-Ti oxide pairs microprobe geochemistry. See data in Table 5. NNO—nickel-nickel-oxide.

mid-Tertiary red continental deposits described in other places of central Mexico, such as the upper part of the Conglomerado Rojo of Guanajuato Formation, apparently of Eocene age (Edwards, 1955; Echegoyén et al., 1970). Furthermore, the contact between Guanajuato's red conglomerate with overlying green Loseros Formation (Echegoyén et al., 1970) is similar to the succession of continental red sandstones and Cerro Azul epiclastic deposits of the Bernal area. The ignimbrites include sanidine, quartz, and minor biotite, and they can be correlated with similar 30–31 Ma ignimbrites reported nearby and to the WNW of the Bernal area and next to, but unrelated to, the Amazcala caldera (Aguirre-Díaz and López-Martínez, 2001).

San Martín andesite was derived from the neighboring San Martín volcano 3 km to the west of Bernal (Fig. 4). It was dated at 11–10 Ma (Table 1) and is one more of several middle Miocene andesitic stratovolcanoes at the north-central border of the Mexican Volcanic Belt, including San Pedro, Palo Huérfano, Chichimequillas, La Joya, and El Zamorano (Valdez-Moreno et al., 1998; Verma and Carrasco-Núñez, 2003; Aguirre-Díaz, 2008).

El Zamorano volcano includes a spine-type lava dome in its crater that is similar to the Peña de Bernal. It is a light-gray, porphyritic rock, almost completely crystalline, and with phenocrysts of plagioclase, hornblende, and quartz. Dome foliation jointing varies from vertical at the central part of the dome to subhorizontal and inward dipping at the borders, similar to the foliation observed in Peña de Bernal. The dacitic dome intrudes and is in high angular unconformity with surrounding outward-dipping lavas of the crater of the El Zamorano volcano. With an altitude of 3360 m above sea level, this spine forms the highest point of the El Zamorano volcano, which is also the highest peak of the State of Querétaro.

Peña de Bernal dacite is interpreted in this work as a lava dome with intrusive contacts with the adjacent rocks. This interpretation is based upon the porphyritic texture and fabric of the rock and the dome-type foliation geometry (e.g., Duffield et al., 1995). A thermal aureole is not present in country rock surrounding the Peña de Bernal dome. The slight metamorphism of Las Trancas Formation was caused by the earlier regional tectonic event of the Laramide orogeny (Suter, 1987) and not by the intrusion of Peña de Bernal dome.

Peña de Bernal dacite dome is intensively fractured along its margins, but it is not brecciated. Shearing of Peña de Bernal dacite along the contact surface formed an intensively fractured rock along some margins, and vertical slickensides were also observed in some places due

TABLE 6. CALCULATED TEMPERATURE (T) AND OXYGEN FUGACITY (fO_2) FOR PEÑA DE BERNAL SAMPLES

Pair	Log fO_2	T (°C)
01	–15.53	711
02	–27.70	377
03	–22.75	444
04	–25.56	430
05	–22.67	377
06	–22.65	445
07	–20.38	512
08	–14.60	747
09	–24.76	391
10	–22.76	443
11	–23.54	431
12	–25.46	381
13	–15.51	718
14	–23.26	437
15	–14.76	766

Note: Mineral microprobe analyses of Fe-Ti oxides analyzed at Paris 6 University-Jussieau Place, by G. Aguirre-Díaz.

to this shearing. These observations, together with the highly crystallized nature of the rock, suggest a forceful intrusion of the dome when it was nearly solid (80% crystalline) and relatively cold (Fig. 16). This is confirmed by geothermometry obtained by microprobe analyses on minerals, which yielded temperatures as high as 711 °C and as low as 377 °C, following the hematite-magnetite buffer (Fig. 15). Therefore, the crystal-rich dacitic magma was almost totally crystallized and relatively cold when it was emplaced at or near surface.

Peña de Bernal dacite was formed through three simultaneous pulses, each constructing a plug; these are the Main plug forming Peña de Bernal peak, the Tortuga plug, and the Northern plug. The Tortuga and Northern plugs are much smaller than the main one. There is no evidence for magmas reaching a vent and flowing over the surface as lava coulees. Instead, Peña de Bernal dacite was emplaced as an endogenous lava dome; that is, the dome grew as a dacitic magma batch that was emplaced and cooled below but near surface.

In summary, Peña de Bernal dacite was apparently intruded as a spine dome, following Blake's (1990) classification, and it probably has retained its peculiar steep peak shape since its formation. However, in the case of Peña de Bernal, the spine dome did not form inside a crater of a volcano, as normally occurs in similar cases, for instance, El Zamorano, Sangangüey, or Tequila volcanoes (Nelson and Carmichael, 1984; Wallace and Carmichael, 1994). Instead, Peña de Bernal was emplaced through a marine Mesozoic sedimentary sequence, and without any evident relationship with a preexisting volcano. There is no evidence that Peña de Bernal vented to the surface, either in volcanic deposits of appropriate age or in dikes that might have fed surface eruptions. The presence of Miocene, relatively intact volcanoes nearby, such as El Zamorano and San Martin, suggests that erosion would not have removed a volcanic edifice above Peña de Bernal dacite, if such had existed.

CONCLUSION

Peña de Bernal is a prominent igneous peak, and it emphasizes the particular geographic and cultural setting where it lies, at the entrance of UNESCO's *Sierra Gorda Biosphere Reserve*, as part of UNESCO's *Intangible Cultural Heritage Patrimony List*, and next to the *Magic Town* of Bernal. With a measured height of 433 m from its base, it is apparently the highest monolith in the world. Peña de Bernal includes three plugs with a general N40°E trend and covers an area of ~4.8 km^2. We conclude that Peña de Bernal was emplaced as a spine-type, endogenous dome, at ca. 8.7 ± 0.2 Ma. Compositionally it corresponds to a dacitic lava with SiO_2 = 67 wt% and $Na_2O + K_2O$ = 6 wt%. The rock is 80 vol% crystalline and only 20 vol% glass. It is porphyritic with plagioclase, pyroxene, hornblende, biotite, quartz, magnetite, ilmenite, apatite, and zircon. On the basis of temperatures as low as 377 °C, the nearly crystalline texture, and the fragile intrusion observations, such as slickensides at the contact with the country rock, it is concluded that Peña de Bernal rock was emplaced by forceful intrusion when nearly solid.

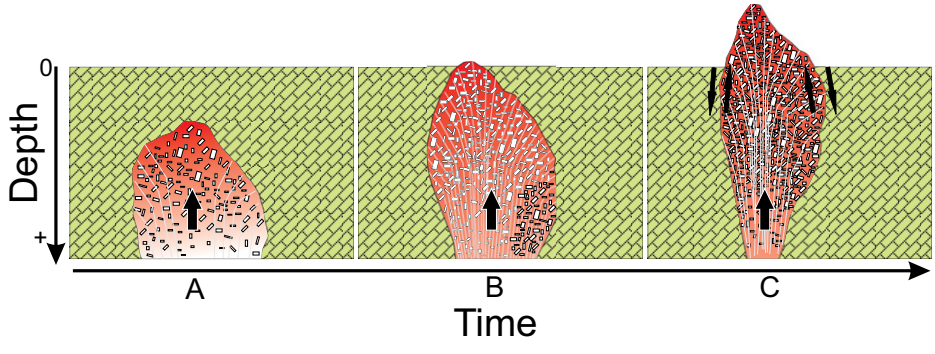

Figure 16. Schematic model showing the emplacement evolution of Peña de Bernal dome, from (A) intrusion of a dacitic magma body at depth, (B) ascent and crystallization of magma body to form an endogenous lava dome near the surface, and (C) forceful intrusion of a nearly solid plug as a spine-type lava dome. From A to B, the magma is richer in crystal content, reaching 80 vol% in the last stage when it completely cools down. Concentric dome foliation typical of endogenous lava domes is indicated by the vertical to subhorizontal white light lines.

ACKNOWLEDGMENTS

We thank the reviewers Don F. Parker, Fred W. McDowell, and Geosphere's associate editor Megan Elwood Madden and science editor Carol Frost for their comments and recommendations that substantially improved the final version. We are grateful to Isaac A. Farraz-Montes and Azalea J. Ortiz-Rodríguez for their help with figures and digital elevation data analysis. We thank Compañía Minera Peña de Bernal, S.A. de C.V. for allowing the use of some data from the unpublished internal report Estudio geológico-estratigráfico y estructural, en el área del proyecto San Martín performed in 2006 by researchers of Universidad Autónoma de San Luis Potosí (UASLP). We thank Andrea Di Muro for arranging access to the microprobe of the Laboratoire de Pétrologie Modélisation des Matériaux et Processus, of Universite Pierre et Marie Curie, Paris 6, France. This work was partially supported by Consejo Nacional de Ciencia y Tecnología (CONACYT) and Programa de Apoyo a Proyectos de Investigación e Innovación Tecnológica–Universidad Nacional Autónoma de México (PAPIIT-UNAM) grants to the first author, numbers IN-114606, IN-106109, IN-112312, P-46005F and 33084T.

REFERENCES CITED

Aguirre-Díaz, G.J., 2008, Historia volcánica del entorno del valle de Querétaro, *in* Lozano-Guzmán, A., and Arzate, J., eds., El Valle de Querétaro y su Geoentorno, Querétaro: Publicación Especial Consejo Nacional de Ciencia y Tecnología del Estado de Querétaro [CONCYTEQ], Querétaro, México y Centro de Geociencias, UNAM-Juriquilla, p. 27–43.

Aguirre-Díaz, G.J., and López-Martínez, M., 2001, The Amazcala caldera, Querétaro, central Mexican Volcanic Belt, México: Geology and geochronology: Journal of Volcanology and Geothermal Research, v. 111, p. 203–218, doi:10.1016/S0377-0273(01)00227-X.

Aguirre-Díaz, G.J., Ferrari, L., Nelson, S.A., Carrasco-Núñez, G., López-Martínez, M., and Urrutia-Fucugauchi, J., 1998, El Cinturón Volcánico Mexicano: Un Nuevo Proyecto Multidisciplinario: Unión Geofísica Mexicana: Geos, v. 18, p. 131–138.

Aguirre-Díaz, G.J., Labarthe-Hernández, G., Tristán-González, M., Nieto-Obregón, J., and Gutiérrez-Palomares, I., 2008, *in* Gottsmann, J., and Martí, J., eds., Ignimbrite Flare-Up and Graben-Calderas of the Sierra Madre Occidental, Mexico, Caldera Volcanism: Analysis, Modelling and Response: Amsterdam, Elsevier, Developments in Volcanology, v. 10, p. 143–180.

Andersen, D.J., Lindsley, L.D.H., and Davidson, P.M., 1993, QUILF, A Pascal program to assess equilibria among Fe-Mg-Mn-Ti oxides, pyroxenes, olivine, and quartz:

Computers & Geosciences, v. 19, p. 1333–1350, doi: 10.1016/0098-3004(93)90033-2.

Bartolini, C., Wilson, J.L., and Lawton, T.F., eds., 1999, Mesozoic Sedimentary and Tectonic History of North Central Mexico: Boulder, Colorado, Geological Society of America Special Paper 340, 380 p.

Bellon, H., Quoc-Buü, N., Chaumont, J., and Philippet, J.C., 1981, Implantation ionique d'argon dans une cible support: Application au traçage isotopique de l'argon contenu dans les minéraux et les roches: Les Comptes Rendus de l'Académie de Paris, v. 292, p. 977–980.

Blake, S., 1990, Viscoplastic models of lava domes, *in* Fink, J. H., ed., Lava Flow and Domes: Emplacement, Mechanisms and Hazard Implications: Berlin, Springer-Verlag, p. 88–126.

Carrillo-Martínez, M., 1990, Geometría estructural de la Sierra Madre Oriental entre Peñamiller y Jalpan, Estado de Querétaro: Sociedad Geológica Mexicana, Convención Geológica Nacional, 6, México, D.F., Libro-guía de la excursión geológica a la región de Zimapán y áreas circundantes, Estados de Hidalgo y Querétaro, p. 1–20.

Carrillo-Martínez, M., 1998, Hoja Zimapán, Carta Geológica de México Serie 1:100,000, Hoja 14Q-e(7): Instituto de Geología, Universidad Nacional Autónoma de México, 1 sheet.

Carrillo-Martínez, M., and Suter, M., 1990, Tectónica de los alrededores de Zimapán, Hidalgo y Querétaro: Sociedad Geológica Mexicana, Convención Geológica Nacional, 6, México, D.F., Libro-guía de la excursión geológica a la región Zimapán y áreas circundantes, estados Hidalgo y Querétaro, p. 1–20.

Cerca-Martínez, L.M., Aguirre-Díaz, G., and López-Martínez, M., 2000, The geologic evolution of southern Sierra de Guanajuato, México: A documented example of the transition from the Sierra Madre Occidental to the Mexican Volcanic Belt: International Geology Review, v. 42, p. 131–151, doi:10.1080/00206810009465073.

Chauve, P., Fourçade, E., and Carrillo-Martínez, M., 1985, Le raports stucturaux entre les domaines cordillérain et mésogéen dans la partie centrale du Mexique: Les Comptes Rendus de l'Académie de Paris, v. 301, p. 335–340.

Coenraads, R.R., and Koivula, J.I., 2007, Earth's dynamic forces: Helenora Heights, Australia, Geologica, Millennium House Pty. Ltd., 576 p.

Cotten, J., Le Dez, A., Bau, M., Caroff, M., Maury, R., Dulski, P., Fourçade, S., Bohn, M., and Brousse, R., 1995, Origin of anomalous rare-earth element and yttrium enrichments in subaerially exposed basalts: Evidence from French Polynesia: Chemical Geology, v. 119, p. 115–138, doi:10.1016/0009-2541(94)00102-E.

Demant, A., 1978, Interpretación geodinámica del volcanismo del Eje Neovolcánico Transmexicano: Revista Mexicana de Ciencias Geológicas, v. 5, p. 217–222.

Duffield, W.A., Richter, D.H., and Priest, S.S., 1995, Physical volcanology of silicic lava domes as exemplified by the Taylor Creek Rhyolite, Catron and Sierra Counties, New Mexico: U.S. Geological Survey Map I-2399, scale 1:50,000.

Echegoyén, J., Romero-Martínez, S., and Velázquez-Silva, S., 1970, Geología y yacimientos minerales de la parte central del distrito minero de Guanajuato: Boletín Consejo de Recursos Minerales no Renovables, v. 75, 35 p.

Edwards, D.J., 1955, Studies of some early Tertiary red conglomerates of central Mexico: U.S. Geological Survey Professional Paper 264-H, p. 153–185.

INAH, 2009, Instituto Nacional de Antropología e Historia, México: Official web page www.inah.gob.mx, note retrieved on September 9, 2009.

INEGI, 2002, Carta topográfica escala 1:50,000, CD con datos vectoriales, Datum: ITRF92 Elipsoide: GRS80, Cartas F14C57 y F14C67.

Labarthe-Hernández, G., Tristán-González, M., and Aranda-Gómez, J.J., 1982, Revisión estratigráfica del Cenozoico de la parte central del Estado de San Luis Potosí: Universidad Autónoma de San Luis Potosí, Instituto de Geología y Metalurgia, Folleto Técnico 85, 208 p.

Le Bas, M.J., Le Maitre, R.W., Streckeisen, A., and Zanettin, B., 1986, A chemical classification of volcanic rocks based on the total alkali-silica diagram: Journal of Petrology, v. 27, p. 745–750, doi:10.1093/petrology/27.3.745.

Lindsley, D.H., and Frost, B.R., 1992, Equilibria among Fe-Ti oxides, pyroxenes, olivine, and quartz: Part I. Theory: The American Mineralogist, v. 77, p. 987–1003.

Lozano-Santacruz, R., and Bernal, J.P., 2005, Characterization of a new set of eight geochemical reference materials for XRF major and trace element analysis: Revista Mexicana de Ciencias Geológicas, v. 22, p. 329–344.

McDowell, F.W., and Clabaugh, S.E., 1979, Ignimbrites of the Sierra Madre Occidental and their relation to the tectonic history of western Mexico: Geological Society of America Special Paper 118, p. 113–124.

Municipio Ezequiel Montes, 2009, Official web page of Municipio de Ezequiel Montes, Querétaro: http://www.queretaro-mexico.com.mx/montes/, retrieved on September 9, 2009.

Nelson, S.A., and Carmichael, I.S.E., 1984, Pleistocene to Recent alkali volcanism in the region of Sanganguey volcano, Nayarit, Mexico: Contributions to Mineralogy and Petrology, v. 85, p. 321–335, doi:10.1007/BF01150290.

Padilla y Sánchez, R.J., 1985, Las estructuras de la Curvatura de Monterrey, Estados de Coahuila, Nuevo León, Zacatecas y San Luis Potosí: Revista Mexicana de Ciencias Geológicas, v. 6, p. 1–20.

Peccerillo, A., and Taylor, S.R., 1976, Geochemistry of Eocene calc-alkaline volcanic rocks from the Kastamonu area, northern Turkey: Contributions to Mineralogy and Petrology, v. 58, p. 63–81, doi:10.1007/BF00384745.

Renne, P.R., Swisher, C.C., Deino, A.L., Karner, D.B., Owens, T.L., and DePaolo, D.J., 1998, Intercalibration of standards, absolute ages and uncertainties in $^{40}Ar/^{39}Ar$ dating: Chemical Geology, v. 145, p. 117–152, doi:10.1016/S0009-2541(97)00159-9.

Segerstrom, K., 1961, Geology of the Bernal-Jalpan Area Estado de Querétaro Mexico: U.S. Geological Survey Bulletin 1104-B, p. 19–82.

Segerstrom, K., 1962, Geology of south-central Hidalgo and northeastern Mexico, Mexico: U.S. Geological Survey Bulletin 1104-C, p. 87–162.

Siebe, C., Macías, J.L., and Aguirre-Díaz, G.J., eds., 2006, Neogene–Quaternary Continental Margin Volcanism: A Perspective from Mexico: Boulder Colorado, Geological Society of America Special Paper 402, 329 p.

Steiger, R.H., and Jäger, C., 1977, Subcommission on Geochronology: Convention on the use of decay constants in Geo and Cosmochronology: Earth and Planetary Science Letters, v. 36, p. 359–362.

Suter, M., 1987, Structural traverse across the Sierra Madre Oriental fold-thrust belt in east-central Mexico: Geological Society of America Bulletin, v. 98, p. 249–264, doi:10.1130/0016-7606(1987)98<249:STATSM>2.0.CO;2.

Tristán-González, M., Aguirre-Díaz, G.J., Labarthe-Hernández, G., Torres-Hernández, J.R., and Bellon, H., 2009, Post-Laramide and pre-Basin and Range deformation and implications for Paleogene (55–25 Ma) volcanism in central Mexico: A geological basis for a volcano-tectonic stress model: Tectonophysics, v. 471, p. 136–152.

UNESCO, 2001, Sierra Gorda (Mexico) and Waterberg (South Africa) join world network of UNESCO biosphere reserves, The MAB United Nations Educational, Scientific and Cultural Organization, UNESCO MAT Program, UNESCO Press, March 2001 issue: http://www.unesco.org/bpi/eng/unescopress/2001/01-46e.shtml (March, 2001).

UNESCO, 2009, Places of memory and living traditions of the Otomí-Chichimecas people of Tolimán: The Peña de Bernal, guardian of a sacred territory, UNESCO Culture Sector, Intangible Heritage: http://www.unesco.org/culture/ich/RL/00174 (September 2009).

Valdez-Moreno, G., Aguirre-Díaz, G.J., and López-Martínez, M., 1998, El Volcán La Joya, Edos. de Querétaro y Guanajuato: Un Estratovolcán antiguo del Cinturón Volcánico Mexicano: Revista Mexicana de Ciencias Geológicas, v. 15, p. 181–197.

Verma, S.P., and Carrasco-Núñez, G., 2003, Reappraisal of the geology and geochemistry of volcán Zamorano, Central Mexico: Implications for discriminating the Sierra Madre Occidental and Mexican Volcanic Belt provinces: International Geology Review, v. 45, p. 724–752, doi:10.2747/0020-6814.45.8.724.

Verma, S.P., Sotelo-Rodríguez, Z.T., and Torres-Alvarado, I.S., 2002, SINCLAS: Standard Igneous Norm and Volcanic Rock Classification System: Computers and Geosciences, v. 28, p. 711–715.

Wallace, P.J., and Carmichael, I.S.E., 1994, Petrology of Volcan Tequila, Jalisco, Mexico: Disequilibrium phenocryst assemblages and evolution of the subvolcanic magma system: Contributions to Mineralogy and Petrology, v. 117, p. 345–361, doi:10.1007/BF00307270.

White, D.E., 1948, Antimony deposits of the Soyatal District, State of Querétaro, Mexico: U.S. Geological Survey Bulletin 960-B, p. 35–88.

Wilcox, R.E., 1979, The liquid line of descent and variation diagrams, *in* Yoder, H.S., Jr., ed., The Evolution of the Igneous Rocks: Princeton University Press, p. 206–232.

Wilson, M., 1989, Igneous Petrogenesis: A Global Tectonic Approach: London, Unwin Hyman, 466 p.

Wilson, B.W., Hernández-M., J.P., and Meave, T.E., 1955, Un banco calizo del Cretácico en la parte oriental del estado de Querétaro: Boletín de la Sociedad Geológica Mexicana, v. 18, p. 1–10.

York, D., Evensen, N.M., López-Martínez, M., and De Basabe-Delgado, J., 2004, Unified equations for the slope, intercept, and standard errors of the best straight line: American Journal of Physics, v. 72, no. 3, p. 367–375.